

The Luminosity Function of Galaxies in Compact Groups ¹

Sally D. Hunsberger and Jane C. Charlton²

Astronomy & Astrophysics Department

Pennsylvania State University

University Park, PA 16802

sdh@astro.psu.edu

charlton@astro.psu.edu

and

Dennis Zaritsky³

UCO/Lick Observatories and Astronomy & Astrophysics Department,

University of California, Santa Cruz, CA 95064

dennis@ucolick.org

To be published in *The Astrophysical Journal*

ABSTRACT

From R-band images of 39 Hickson compact groups (HCGs), we use galaxy counts to determine a luminosity function extending to $M_R = -14.0 + 5 \log h_{75}$, approximately two magnitudes deeper than previous compact group luminosity functions. We find that a single Schechter function (Schechter 1976) is a poor fit ($\chi^2_\nu > 4$) to the data, so we fit a composite function consisting of separate Schechter functions for the bright and faint galaxies. The bright end is best fit with $M^* = -21.6$ and $\alpha = -0.52$ and the faint end with $M^* = -16.1$ and $\alpha = -1.17$. The decreasing bright end slope implies a deficit of intermediate luminosity galaxies in our sample of HCGs and the faint end slope is slightly steeper than that reported for earlier HCG luminosity functions. Furthermore, luminosity functions of subsets of our sample reveal more substantial dwarf populations for groups with x-ray halos, groups with tidal dwarf candidates, and groups with a dominant elliptical or lenticular galaxy. Collectively, these results support the hypothesis that within compact groups, the initial dwarf galaxy population is replenished by “subsequent generations” formed in the tidal debris of giant galaxy interactions.

Subject headings: galaxies — luminosity function, compact groups, evolution

¹Observations were made on the 60 inch telescope at Palomar Mountain, which is jointly operated by the California Institute of Technology and the Carnegie Institution of Washington.

²Center for Gravitational Physics and Geometry, Pennsylvania State University

³Alfred P. Sloan Research Fellow

1. Introduction

The dwarf galaxy population is not merely an extension of giants to fainter luminosities. Fundamental differences between the two populations raise the issue of whether the same formation mechanism applies to both. Understanding the origin and evolution of dwarf galaxies is essential in developing the correct model of galaxy and cluster formation. Because compact groups are unique environments and active sites of galaxy interaction, they provide an opportunity to study the formation of dwarf galaxies both as a function of environment and in tidal debris.

Hickson (1982) cataloged 100 compact groups of galaxies, selecting them on the basis of population, isolation, and compactness. Radial velocity measurements (Hickson et al. 1992) and morphological studies (Mendes de Oliveira & Hickson 1994) suggest that most of the Hickson compact groups (HCGs) are physical associations, although Mamon (1990) has argued that the data are also consistent with many HCGs being superpositions of binary-rich loose groups and Hernquist et al. (1995) contend that many compact groups are chance projections of large filamentary structures. Diaferio et al. (1994) propose that during the collapse of a rich loose group of galaxies, compact configurations are continuously forming and that the members of such a compact group eventually merge, even as new galaxies are joining the group from the surrounding region.

Regardless of the exact fraction of groups that are physical associations, compact groups are sites of galaxy interactions and among themselves, they provide a variety of environments to examine (e.g., x-ray luminous vs. non-luminous, elliptical vs. spiral dominated,

tidally interacting vs. quiescent). Compact groups are particularly intriguing because of the combination of high galaxy projected density (similar to the centers of rich clusters) and low velocity dispersion (comparable to loose groups). This combination suggests, at least for the fraction of physical groups, that interactions and mergers occur frequently and that during such encounters, tidal forces have sufficient time to extract significant amounts of material, resulting in tidal tails and bridges. As proposed by Zwicky (1956), self-gravitating objects might develop in tidal tails and evolve into dwarf galaxies. This idea is supported by the observation of regions of active star formation at the ends of tidal tails in the Superantennae and Antennae systems (Mirabel et al. 1991, Mirabel et al. 1992) and of two dwarf galaxies in the tidal tails of Arp 105 (Duc & Mirabel 1994). Furthermore, numerical simulations (Barnes & Hernquist 1992, Elmegreen et al. 1993) confirm that gravitationally bound clumps can form in tidal tails. Therefore, compact groups represent a unique environment in which to study the formation of dwarf galaxies in tidal debris. In a previous paper (Hunsberger et al. 1996), we examined a sample of 42 HCGs and identified 47 tidal dwarf candidates in seven groups with tidal tails and tidal arms. We also estimated the fraction of compact group dwarf galaxies produced by the tidal dwarf formation mechanism over the lifetime of a group and found it to be significant ($> 30\%$).

Previously determined luminosity functions of compact groups (Heiligman & Turner 1980, Mendes de Oliveira & Hickson 1991, Sulentic & Rabaça 1994, Ribeiro et al. 1994, Zepf et al. 1997) have yielded faint end slopes of $\alpha = 0.0$, $\alpha = -0.2 \pm 0.9$, $\alpha = -1.13 \pm 0.13$, $\alpha = -0.82 \pm 0.09$, and $\alpha = -1.0$, respec-

tively. Some of these values are flatter than that observed in either clusters ($-1.4 < \alpha < -1.0$; Ferguson & Sandage 1991) or the field ($\alpha \sim -1.0$; Loveday et al. 1992, Marzke et al. 1994, Ratcliffe et al. 1998) implying fewer dwarfs per giant in compact groups than in the other environments. The Heiligman & Turner (1980) luminosity function used ten compact groups (not necessarily HCGs) for which galaxy redshifts were available at that time. Knowing the completeness limits of the Palomar Sky Survey from which the groups were identified, they quantified the deficit of fainter members in their sample by a comparison to the field luminosity function. The number of “missing” galaxies was significant and could not readily be attributed to small sample size, inaccurate photometry, galaxy misclassification, or selection effects. Using a sample of 68 HCGs, Mendes de Oliveira & Hickson (1991) determined the “best-fit” parameters of their luminosity function with Monte Carlo simulations of compact groups selected from various Schechter distributions. They similarly concluded that there is a lack of low luminosity galaxies due to environmental factors rather than selection effects and suggested that the excess of very luminous ellipticals (the mean magnitude of HCG ellipticals is brighter than that of Virgo cluster ellipticals) coupled with a deficit of fainter galaxies indicates merger activity. Sulentic & Rabaça (1994) extended the compact group luminosity function to fainter absolute magnitudes using the Hickson catalog but applying a correction factor for incompleteness. Although their adopted value for the faint end slope did not reflect the decreasing number of low luminosity galaxies of previous luminosity functions, they noted that a single Schechter function did not provide a good fit to both bright and faint ends simultaneously. Ribeiro

et al. (1994) obtained CCD images of 22 HCGs and used a statistical method to create a luminosity function which probed the galaxy population fainter than the original Hickson catalog, however, the resultant compact group luminosity function did not reveal the depletion of faint galaxies suggested by earlier analyses. Zepf et al. (1997) confirmed the validity of this photometric approach by obtaining spectroscopic redshifts and producing a similar luminosity function.

Most luminosity functions are presented as averaged functions and do not address questions arising from environmental differences and tidal dwarf formation. In this paper, we present luminosity functions determined by a statistical technique, similar to that used by Ribeiro et al. (1994), to address issues regarding dwarf galaxy formation. The technique involves using galaxy counts in the outer regions of images to statistically subtract the background/foreground contribution. Such an approach bypasses the need to obtain redshifts of all faint galaxies within the compact group field; so only moderately deep imaging is required. Using galaxy counts within 17 HCGs, the Zepf et al. (1997) luminosity function extends down to $M_B = -14.5 + 5 \log h$. Our luminosity function uses a sample of 39 HCGs and extends to $M_R = -13.4 + 5 \log h$ ($M_R = -14.0 + 5 \log h_{75}$). Therefore, our limit is two magnitudes fainter assuming a typical dwarf galaxy color of $B - R = 1.0$, which is the median value for Local Group dwarf galaxies⁴. We compare luminosity functions of various sub-samples of HCGs such as spiral-dominant

⁴From NED, the NASA/IPAC Extragalactic Database is operated by the Jet Propulsion Laboratory, California Institute of Technology, under contract with the National Aeronautics and Space Administration.

vs. elliptical-dominant, x-ray-rich vs. x-ray-poor, and groups with tidal dwarfs vs. groups without tidal dwarfs to discover how processes such as galaxy destruction, galaxy creation, and tidal stripping modify the luminosity function of a compact group during its evolution.

In the next section (§2), we describe the observational procedures and data analysis. The method for determining a luminosity function is detailed in §3 and we present the results in §4. In §5 the major results are summarized and discussed and we present some speculations as to the origin of the luminosity function differences.

2. Data Acquisition and Analysis

We selected compact groups from the Hickson catalog (1982) on the basis of their angular size and the apparent magnitudes of member galaxies (Hickson 1982, Hickson et al. 1989). To ensure that the groups fit well within the field-of-view, we selected those with angular diameters $< 7'$. In redshift, we chose groups with $z \leq 0.05$ so that objects as faint as $M_R > -16$ (well into the regime of dwarf galaxies) were above our detection limit. For a typical redshift, $z = 0.03$ or $cz = 9000 \text{ km s}^{-1}$, our median limiting apparent magnitude of 21.3 corresponds to $M_R = -14.1$ (using $H_0 = 75 \text{ km s}^{-1} \text{ Mpc}^{-1}$, $q_0 = 0.1$). Of the 66 Hickson compact groups that satisfied these criteria, 49 are observable in November from Palomar.

We obtained Johnson R-band images of 39 Hickson compact groups (listed in Table 1) using the 1.5-m telescope at Palomar. A thinned Tektronix 2048×2048 CCD was binned by 2 in both directions and provided a $12.8' \times 12.8'$ field-of-view with $0.75''/\text{pixel}$. Over four nights, two 15-minute exposures

were taken of each group. Offset frames, positioned $10'$ from the group center, were also taken for 18 HCGs in our sample. Calibration frames (5-minute exposures of each compact group) and standard star fields (Landolt 1992) were obtained during the fifth night under photometric conditions.

The data were reduced using IRAF⁵. A median of 44 bias frames was subtracted from each image. The median of 55 images, including standard star fields, calibration frames, and offset frames (taken $10'$ from the group center), was used to flat field images because it produced a smoother background than either twilight or dome flats. Next, we removed bad pixels and cosmic rays, combined the two 15-minute images of each group, and calibrated the images using the 5-minute photometric exposures and standard stars observed at a range of airmasses.

Our standard star reductions indicated that there was a slight color term between the Landolt (1992) system and our observations. For dwarf galaxies (which are the primary focus of this study), a typical color of $(B - R) = 1.0$, yielded a color term error of only 0.01 magnitudes. There was no color information available for our dwarf candidates, so we omitted this apparently insignificant correction. Our standard star calibration uncertainties were ~ 0.02 magnitudes.

We used FOCAS (Faint Object Classification and Analysis System) (Jarvis & Tyson 1981) to identify non-stellar objects in the images. The software generated a catalog of objects on the basis of user-defined detection

⁵IRAF is distributed by the National Optical Astronomy Observatories, which are operated by the Association of Universities for Research in Astronomy, Inc. (AURA) under cooperative agreement with the National Science Foundation.

parameters. We required that objects have at least six contiguous pixels 1.75σ above the local background. These values were set interactively to include low surface brightness dwarf candidates that were apparent by visual inspection. FOCAS computed a significance statistic for each object, which we used as a detection criterion. By examining detected objects and their significance, we defined our lowest acceptable significance value to be 1.0. Those objects classified as galaxies (i.e., extended) were included in our galaxy counts.

3. Determination of a Luminosity Function

A simple statistical technique is used to determine the luminosity function. For each CCD frame, regions are selected that define the projected area of a compact group and the surrounding background (Figure 1). The magnitude distribution of FOCAS-detected galaxies in the background region allows us to predict the contribution of foreground and background objects to galaxy counts observed at each magnitude interval within the compact group area. By subtracting background counts from total counts, we estimate a magnitude distribution which is representative of the compact group galaxies without determining group membership for individual objects in the field. Because of the statistical nature of this method, it is most effective when data are combined from many images (the sample is presented in Figures 2a through 2g). The details of our procedure are described below.

The compact group area on each image is defined in terms of a group radius. The area of the group is determined by first finding the smallest circle enclosing the positions of every member with an accordant velocity.

Galaxies which have relative radial velocities within 1000 km/s are said to have accordant velocities and are presumed to be physically associated (Hickson et al. 1992). Some members originally cataloged by Hickson (1982) have discordant velocities, implying that they are foreground/background galaxies and we omit them from the group. While the group center remains fixed, the circle is expanded to include surface brightness contours of $R = 23$ mag/arcsec² around each member so that the entire galaxy is considered part of the group. This procedure defines the group radius, R_G . A background area is defined as that region beyond twice the group radius extending almost to the edges of the CCD image. Galaxy counts from the outer regions of 34 CCD images are combined to create a “background” magnitude distribution. Because the limiting magnitude is different for each frame, the faintest magnitude bins are determined by fewer frames and must be corrected so that the counts in each bin correspond to equal areas.

The resultant background is compared to Tyson’s galaxy counts (Tyson 1988) to check that we have extracted an appropriate representation of the field luminosity function from our data (Figure 3a). We find the following deviations of the HCG background from Tyson’s counts: there is an absence of bright galaxies ($R < 14.0$) and an excess in some of the fainter bins ($R = 18.5, 19.5$). The lack of bright galaxies is readily explained by one of Hickson’s original selection criteria: between one and three group radii, there can be no galaxies brighter than the brightest group member. The result reported by Ramella et al. (1994), that many compact groups are embedded in rich looser systems, may be responsible for the excess counts ob-

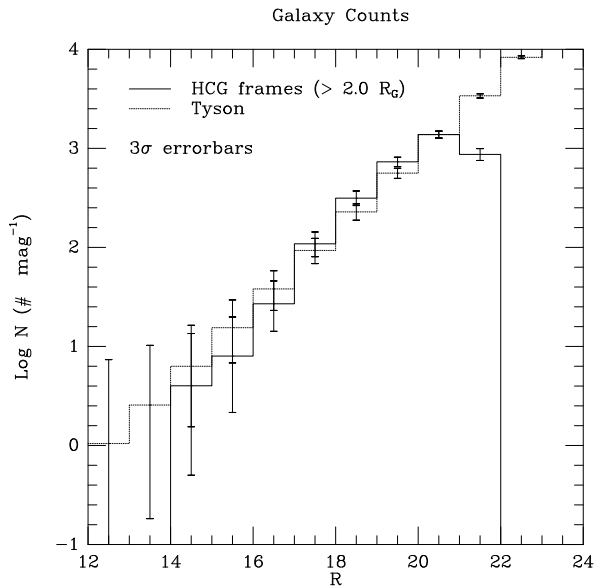


Fig. 3a.— BACKGROUND GALAXY COUNTS. Background galaxy counts using HCG frames are compared to Tyson’s counts. Counts per magnitude interval are plotted as a function of apparent magnitude (R). The expected counts from Tyson’s equation (Tyson 1988) are adjusted to the same area as the background.

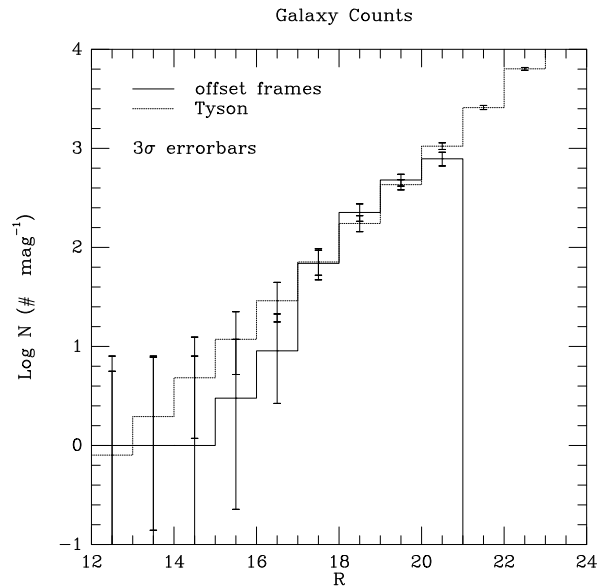


Fig. 3b.— BACKGROUND GALAXY COUNTS. Background galaxy counts using offset frames are compared to Tyson’s counts. Counts per magnitude interval are plotted as a function of apparent magnitude (R). The expected counts from Tyson’s equation (Tyson 1988) are adjusted to the same area as the background.

served in the fainter bins of our background. To confirm that these deviations are not a problem with our FOCAS detection parameters, we compare Tyson’s counts to those of our “offset” frames. The offset frames, taken at Palomar during the same run, are single 15-minute exposures positioned $10'$ from the compact group center. The background created from 18 offset frames is more similar to Tyson’s counts (Figure 3b) and we conclude that the FOCAS detection procedures are sound, although even the offset frames may still sample the surrounding loose group because they overlap the HCG frames by $\sim 2.8'$. If we overestimate the background counts due to this contamination, we will underestimate the number of dwarf members. We could use offset frames that are widely

separated from the group to get better agreement with Tyson’s counts, but they might not properly sample the background at the position of the group.

For each group, the background magnitude distribution is converted to absolute magnitudes using the redshift of the group. The area in which the background contributes must also be defined. We take into account that the background cannot be detected in regions covered by giant group members. Also, we visually examine each group and classify some FOCAS-detected objects as HII regions. Within eleven groups, we omit a total of 31 small, bright objects located along spiral arms. In addition, there are three groups containing four large face-on spirals which exhibit very clumpy substructure and FOCAS

mistakenly identifies this as several individual objects. We eliminate such areas from the group analysis.

We now determine the contribution of group members to the galaxy counts within each compact group area and combine the data from all groups to produce a luminosity function of HCG galaxies. The counts in each absolute magnitude interval represent the average number of galaxies per compact group, although not every group contributes to the fainter bins because of incompleteness. To estimate the completeness of each image, detected objects are binned by apparent magnitude and the faintest bin with counts within $1\sigma(\sqrt{n})$ of the peak of the distribution defines the completeness limit. Table 1 lists the limiting apparent magnitude R of each frame and the corresponding absolute magnitude limit at the redshift of each group.

How well do the FOCAS magnitudes of the bright members agree with the photometric catalog of Hickson et al. (1989)? Of 182 original group members (including those galaxies that were later discovered to have discordant velocities), 172 galaxies are detected but 68 of these have saturated pixels in the central region. Disturbed morphologies and superpositions of stars or other galaxies are the primary causes of non-detection. Using the remaining objects, the median difference between the total galaxy magnitudes calculated from fluxes returned by FOCAS and magnitudes computed from information in the catalog is $\Delta M_R = 0.06$, with the Hickson catalog magnitudes usually being brighter. The average difference is $\Delta M_R = -0.01 \pm 0.37$. For completeness, we use the catalog magnitudes to determine the bright end of our luminosity function.

The final critical issue involves a method

of normalization. The “standard” procedure begins with a sample completeness correction, i.e., determining the magnitude at which a sample becomes incomplete. Following the example of Hickson et al. (1989), one can calculate this value by summing the B_T magnitudes of individual galaxies to obtain group magnitudes, plotting a cumulative distribution of those group magnitudes, and then fitting the distribution to the equation

$$N(m) = \frac{2n}{\pi} \arctan[10^{0.6(m-m_0)}]$$

where n is the number of groups, m is a B_T magnitude, $N(m)$ is the number of groups with magnitude $\leq m$, and m_0 represents the magnitude where the data become incomplete. This assumes that compact groups are uniformly distributed in space and one can then express the probability of detecting a group with magnitude m as

$$P(m) = [1 + 10^{1.2(m-m_0)}]^{-1}.$$

Next, the effective volume of each group, i.e., a sphere whose radius is defined by the maximum distance at which a group is detectable, can be calculated:

$$V_i = A \int_0^\infty P(m_i) r^2 dr$$

where V_i is the volume of the i^{th} group, A is the solid angle of the survey, r is distance in Mpc, and $P(m_i)$ is defined previously. A luminosity function is then normalized by dividing galaxy counts for each group by the effective volume and summing the counts from all groups.

Although this method of normalization is used in determining earlier compact group luminosity functions (Mendes de Oliveira & Hickson 1991, Ribeiro et al. 1994), we normalize our luminosity function by simply dividing the galaxy counts in each magnitude

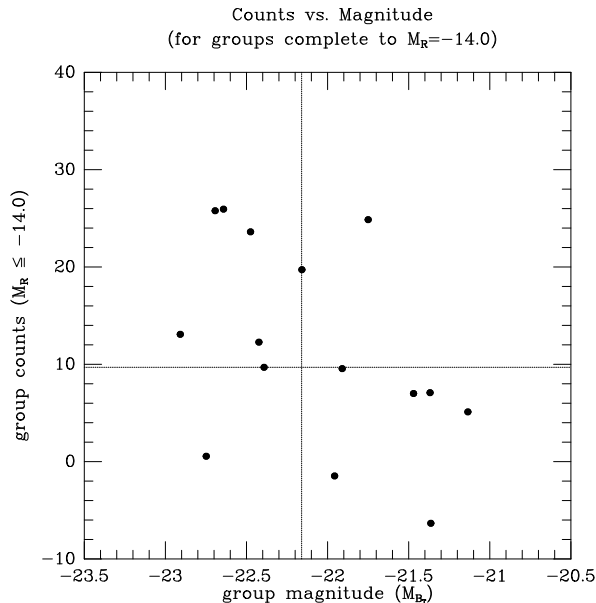


Fig. 4.— GROUP POPULATION VS. GROUP MAGNITUDE. Data points show the number of galaxies brighter than $M_R = -14.0$ for each group within $R = 1.50R_G$ plotted as a function of group magnitude. Tidal dwarf candidates are excluded from the counts. There is a trend for the brightest groups to have the largest population. The confidence level in this correlation is 97.0%. The dotted lines mark the median values.

bin by the number of groups contributing to that bin. We justify this new approach by the following argument. The goal of this study is to develop a luminosity function that reflects the membership of a typical compact group as defined by Hickson, rather than to demonstrate how a hypothetical compact group population defined more generally contributes to the Universal luminosity function. Our method weights galaxy counts from each group equally so that the counts can be averaged. Galaxies identified in more distant groups should not carry less weight. Equal weighting enables us to compare directly the luminosity functions of various groups, for example that of groups with diffuse x-ray emis-

sion to that of groups without emission, when each bin reflects the average number of galaxies expected in a compact group with (or without) that property. The luminosity dependent weighting can also distort the luminosity function if there is a correlation between group luminosity and the dwarf galaxy population. Using a 2×2 contingency table, we find a significant correlation (Figure 4) between group absolute magnitude and number of faint galaxies (the probability of randomly producing a greater or equal correlation is 3%). Such a trend implies that groups having the largest numbers of dwarf galaxies also have the largest effective volumes, and hence the lowest weighting factors. Applying the standard normalization procedure in this situation systematically reduces the dwarf to giant ratio. For this reason, we prefer to measure the number of galaxies per group, rather than per volume.

4. Results

We present a luminosity function of compact group galaxies based on “total” absolute magnitudes in Figure 5. It includes the entire sample of 39 compact groups and the group area is defined by $R = 1.50R_G$, where R_G is the group radius. We adopt this radius because it is the largest area for which all 39 groups are included in their entirety within our images. Each point in our luminosity function graphs represents the number of galaxies per group within a one magnitude interval centered at that point. The errorbars represent 1σ Poisson errors. As the original counts from group and background regions of different frames are combined, errors are propagated by the standard method: $\sigma_z^2 = a^2\sigma_x^2 + b^2\sigma_y^2$, where a and b are numerical constants.

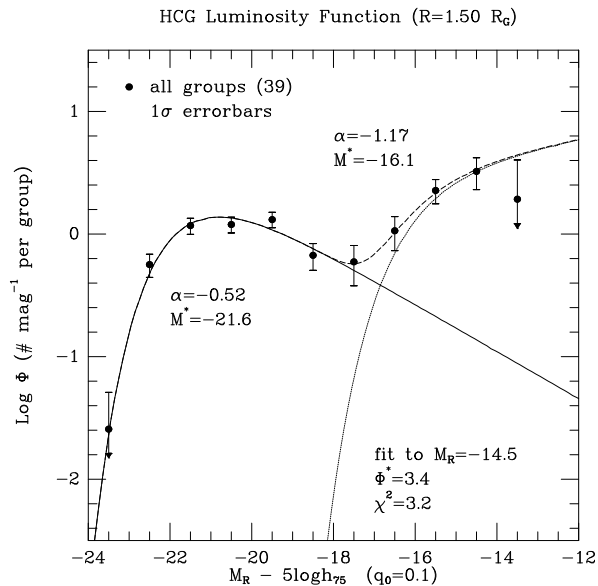


Fig. 5.— LUMINOSITY FUNCTION OF HCG GALAXIES. Data points represent the average number of galaxies per group in each magnitude bin. The bright and faint populations are fit separately using 2 Schechter functions. The solid line is the bright end, the dotted line is the faint end, and the dashed line is the composite fit.

We find that a single Schechter function (Schechter 1976) does not provide a good fit to the data. Using the parameters of the best fit function to define a parent population ($\alpha = -0.72$, $M^* = -21.8$, and $\Phi^* = 2.6$), a χ^2 test gives values of $\chi^2 = 31.2$ with seven degrees of freedom and $P_\chi < .001$ where P_χ is the probability of exceeding χ^2 for a given distribution and its expectation value is 0.50. The result of the χ^2 test indicates very poor agreement between the best fit function and the data. We obtain a much better fit ($\chi^2 = 3.2$ with five degrees of freedom and $P_\chi \sim 0.67$) using the composite of two Schechter functions applied simultaneously to the bright and faint galaxy populations. The best-fit Schechter functions, shown in Figure 5, have slopes of $\alpha = -0.52$ and $\alpha = -1.17$ for the bright and faint ends,

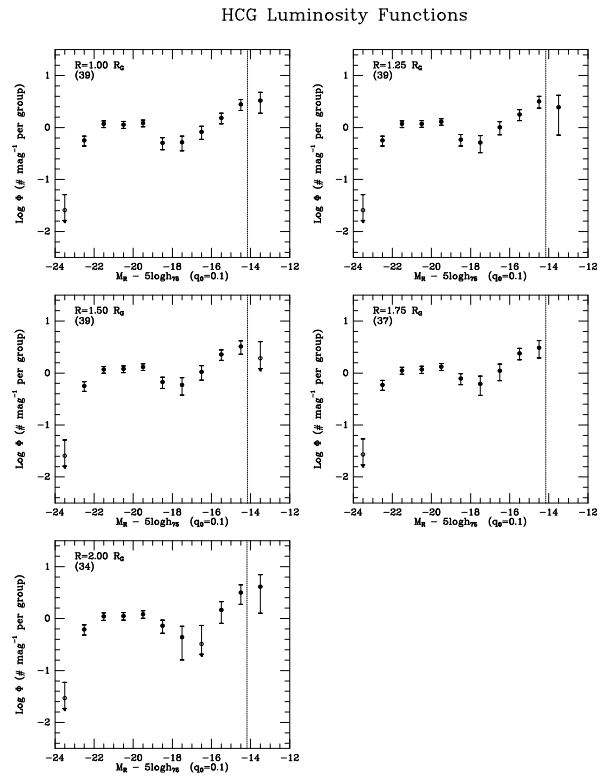


Fig. 6.— LUMINOSITY FUNCTIONS WITHIN DIFFERENT GROUP RADII. The number in parentheses in the upper left corner of each plot is the number of groups in the sample. The vertical lines mark the median completeness for the groups contributing to the luminosity function. An open circle denotes the data point is an upper limit.

respectively.

It is also useful to examine luminosity functions within several radii (Figure 6). The general shape of the luminosity function is similar for all radii: following the data points from bright to faint magnitudes, the bright end begins to fall off beyond $M_R = -19.5$ and continues until $M_R = -16.5$ where there is an upturn. The trough in the luminosity function is unusual, so we examine a few possible explanations. The first possibility is that the background has been overestimated at inter-

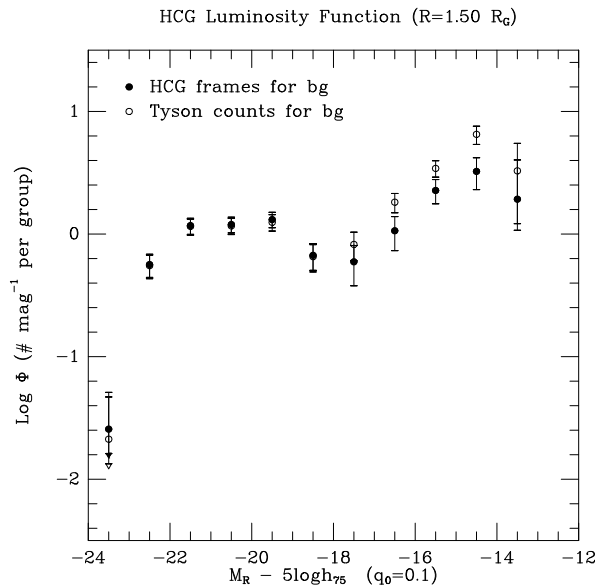


Fig. 7.— COMPARISON OF LUMINOSITY FUNCTIONS USING TYSON’S COUNTS AND HCG FRAMES. This figure shows the difference in using Tyson’s counts and the HCG frames to calculate the number of background galaxies. The HCG background has excess counts (above what is expected from Tyson counts) which leads to fewer compact group galaxies at the faint end of the luminosity function. However, the HCG background may be more representative of regions surrounding compact groups.

mediate magnitudes (recall the excess counts we found relative to Tyson’s counts; Figure 3). When the apparent magnitudes are converted to absolute magnitudes, the magnitude bins in which this excess is present are primarily $M_R \geq -17.5$. Although the trough is lessened when Tyson’s counts are used as the background (Figure 7), it is not completely eliminated and again we emphasize that Tyson’s counts are not necessarily representative of regions surrounding compact groups. The second possibility is that the original selection criteria imposed by Hickson (1982) have led to an observational bias. Recall the

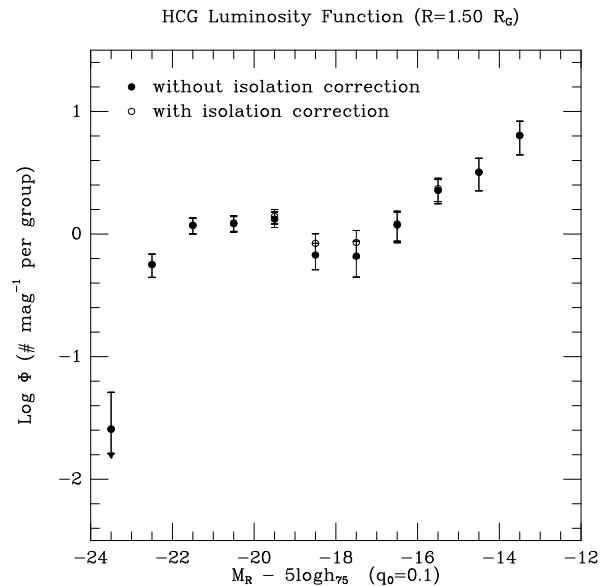


Fig. 8.— COMPARISON OF LUMINOSITY FUNCTIONS WITH AND WITHOUT ISOLATION CORRECTION. This figure shows the effect of Hickson’s original isolation criterion by accounting for the lack of background galaxies within a certain magnitude range. Some counts are recovered in the region of the dip in the luminosity function but isolation is not a major contributor to the deficit of intermediate luminosity galaxies. The background for these luminosity functions is defined as the region beyond 3 group radii instead of 2 group radii in other plots.

isolation criterion: within three group radii, there are no galaxies (other than group members) within three magnitudes of the brightest group member. This means that by definition, the background does not contribute to certain magnitude bins. In order to test this possibility, we create a background using counts beyond three group radii and because there cannot be background galaxies within three magnitudes of the brightest member, we do not subtract a background contribution for those magnitude bins. The corrected luminosity function is shown in Figure 8 and

although the trough is again lessened, it is not removed entirely. The third possibility we consider is that there is incompleteness at these magnitudes because such galaxies are preferentially located near the giant members and so are not detected by FOCAS. Because the deficit at intermediate magnitudes is not seen in certain subsets of the sample, such as groups with x-ray halos and tidal dwarfs, we conclude that there is a genuine deficit of intermediate magnitude galaxies in compact groups relative to the luminosity functions of field and cluster environments.

Because a “group” radius probes different physical distances in different groups, it is valuable to examine luminosity functions with radii defined in terms of kpcs (Figure 9). Again we see the same trends, but the deficit of intermediate galaxies is very evident at 25kpc and gradually becomes less pronounced. This result suggests that the presence of these intermediate galaxies depends on distance from the group center. The dwarf galaxy population ($M_R > -18$) is present at all physical radii.

To examine the relationships between dwarf galaxy evolution and environment, we construct luminosity functions for various group subsets based on the following properties: the existence of tidal dwarf candidates (as determined by Hunsberger et al. 1996), degree of compactness (based on the median separation between giant members; Hickson 1992), estimated mass-to-light ratio (from Hickson 1992), the presence of diffuse x-ray emission (Ponman et al. 1996), projected velocity dispersion of giant members (Hickson 1992), fraction of spiral galaxies (Hickson 1989), type of dominant (first-ranked) galaxy (Hickson 1989), and number of giant members (Hickson 1992). These properties are listed

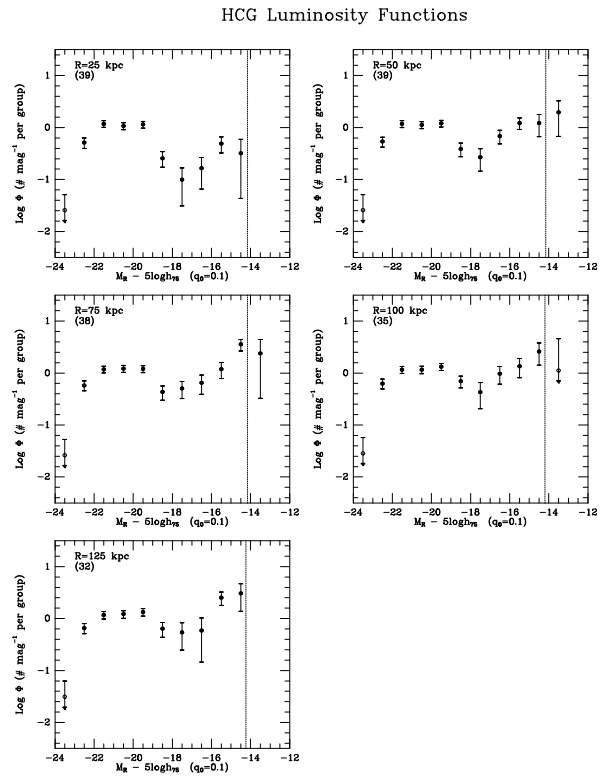


Fig. 9.— LUMINOSITY FUNCTIONS WITHIN DIFFERENT PHYSICAL RADII. The number in parentheses in the upper left corner of each plot is the number of groups in the sample. The vertical lines mark the median completeness for the groups contributing to the luminosity function. An open circle denotes the data point is an upper limit.

for groups in our sample in Table 2:

Column 1 is the group number with * to indicate tidal dwarf candidates and † to indicate diffuse x-ray emission.

Column 2 is the number of giant members with accordant velocities (within 1000 km/s of the group median velocity).

Column 3 gives the morphological type of the first-ranked galaxy.

Column 4 is the spiral fraction of giant members.

Column 5 lists the estimated mass-to-

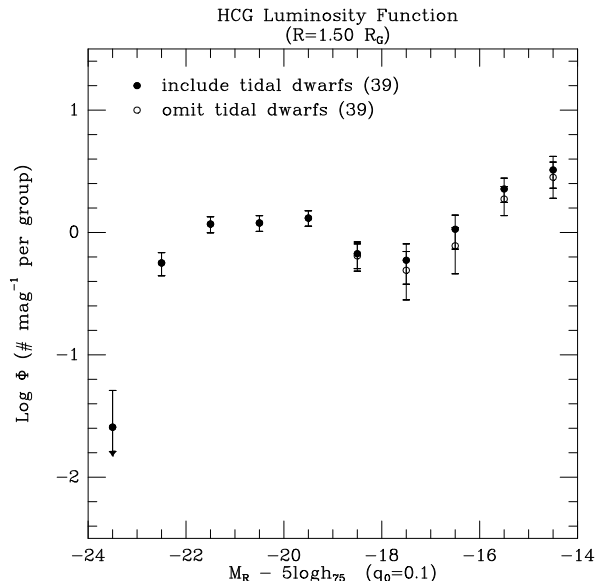


Fig. 10a.— COMPARISON OF LUMINOSITY FUNCTIONS WITH AND WITHOUT TIDAL DWARF CANDIDATES. This plot shows how tidal dwarfs contribute to galaxy counts averaged over all groups. The errorbars for this and subsequent plots are 1σ and an errorbar with an arrow indicates the data point is an upper limit.

light ratio (highly uncertain due to the small number of identified members).

Column 6 lists the projected velocity dispersion.

Column 7 lists the median separation between giant members.

It is impractical to present all these luminosity functions and in many cases, the presence or absence of a particular property does not produce luminosity functions that differ significantly from each other. However, the properties that do substantially impact the shape of the luminosity function are summarized in Figures 10 – 12 and discussed below.

First, we examine the relationship between the presence of tidal dwarfs and the luminosity function. Figure 10a shows that the

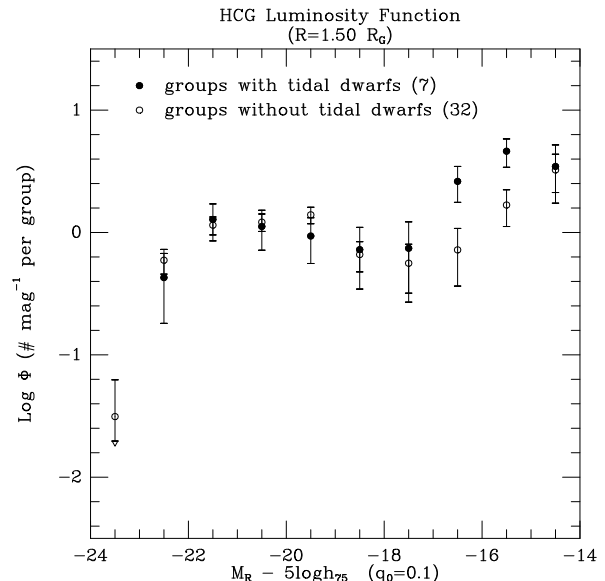


Fig. 10b.— COMPARISON OF LUMINOSITY FUNCTIONS OF GROUPS WITH AND WITHOUT TIDAL DWARF CANDIDATES. One luminosity function is produced by groups which have tidal dwarfs and the other by those which do not have tidal dwarfs. The numbers in parentheses at the top of the plot indicate the number of groups in each subset.

inclusion of tidal dwarf candidates has a negligible impact on the total luminosity function of galaxies in compact groups. Figure 10b illustrates that there is a significant difference at the faint end of luminosity functions for groups with and without tidal dwarfs, but this difference is due *only* to the tidal dwarfs themselves. To simplify the discussion of how other group properties affect the luminosity function, we eliminate tidal dwarf candidates from the galaxy counts in all subsequent luminosity functions.

Second, we examine whether galaxy types of giant group members are correlated with the existence of a dwarf population. If we divide the sample in two, depending on whether the first-ranked galaxy is elliptical/lenticular

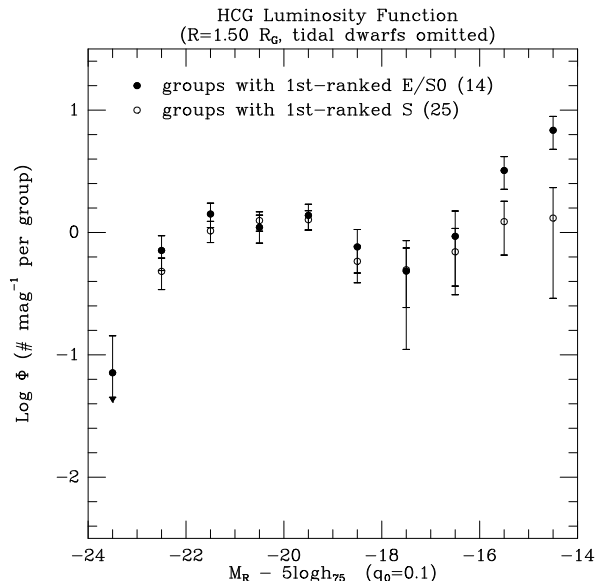


Fig. 11a.— COMPARISON OF LUMINOSITY FUNCTIONS OF GROUPS WITH AND WITHOUT A DOMINANT E/S0 GALAXY. One luminosity function is produced by groups having a first-ranked (dominant) elliptical galaxy and the other by those having a first-ranked spiral. There is an excess of faint galaxies in the groups with a dominant elliptical.

or spiral, we find an excess of dwarf galaxies in the groups with E/S0 first-ranked galaxies (Figure 11a). Furthermore, we note that the faint galaxy population still exists when the compact group area is expanded to two group radii, $R = 2.00R_G$ (Figure 11b) while the intermediate luminosity galaxies are no longer measurable above the background. One possible explanation for the apparent excess of faint galaxies in the E/S0 groups is that these compact groups inhabit a richer environment. However, 9 of the 14 E/S0 dominated groups have backgrounds (counts beyond $R = 2.00R_G$) for which the galaxies per unit area lie below the average of the combined frames. Therefore, the background contribution in the E/S0 groups is, if anything,

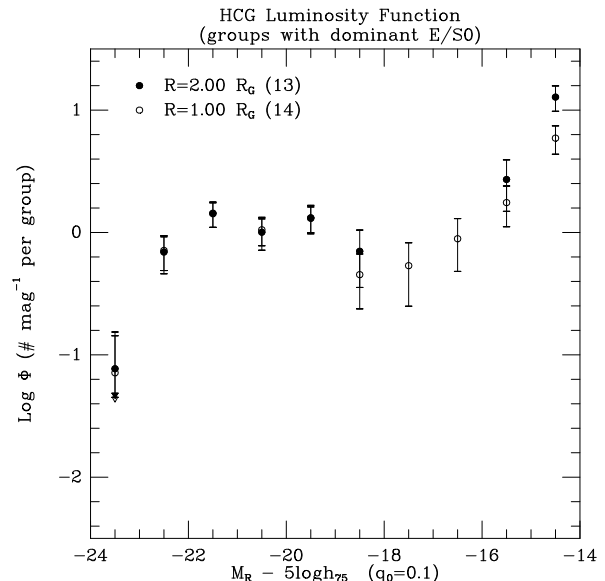


Fig. 11b.— COMPARISON OF LUMINOSITY FUNCTIONS OF DOMINANT E/S0 GROUPS WITHIN DIFFERENT RADII. A dwarf population is still detected when the group region extends to $R = 2.00R_G$, beyond the immediate vicinity of the giant members. The “missing” data points in the plot are caused by negative galaxy counts. When the region is expanded to a large enough distance, the background dominates the galaxy counts and negative values for compact group counts are possible. In this case $\log \Phi$ cannot be plotted.

actually slightly over-estimated, and so we conclude that the faint excess in these groups is associated with the HCGs.

Third, we examine the role of the intergalactic medium. Because diffuse x-ray emission is associated with a hot intra-cluster medium, we divide our sample into groups with and without such x-ray emission based on the results of a ROSAT survey of HCGs (Ponman et al. 1996). Ponman et al. detected diffuse x-ray emission in 22 of 85 groups. Seven of these 22 groups are in our sample and the comparison of luminosity functions of

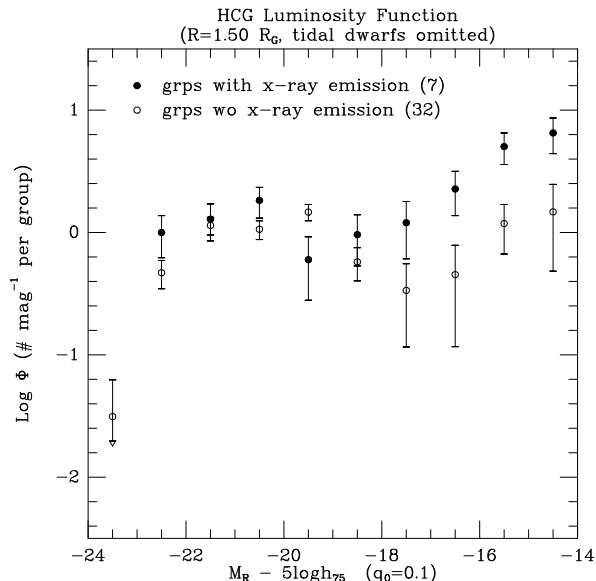


Fig. 12a.— COMPARISON OF LUMINOSITY FUNCTIONS OF GROUPS WITH AND WITHOUT DIFFUSE X-RAY EMISSION. There is an excess of dwarfs in the groups with x-ray halos. Also, the deficit of intermediate galaxies noted in the total luminosity function does not appear for groups with x-ray emission.

groups with and without detected x-ray halos is presented in Figure 12a. Groups with x-ray emission have a substantially larger dwarf population than groups without x-rays. When we compare the luminosity functions of x-ray groups within different radii (Figure 12b), we find that the number of faint galaxies increases with radius.

We infer that for x-ray detected groups, the dwarf population extends to a distance of at least two group radii. Five of the seven x-ray groups also have first-ranked E/S0 galaxies and the other two have tidally interacting members.

In Table 3 we summarize the average galaxy counts for several subsets:

Column 1 describes each subset and the

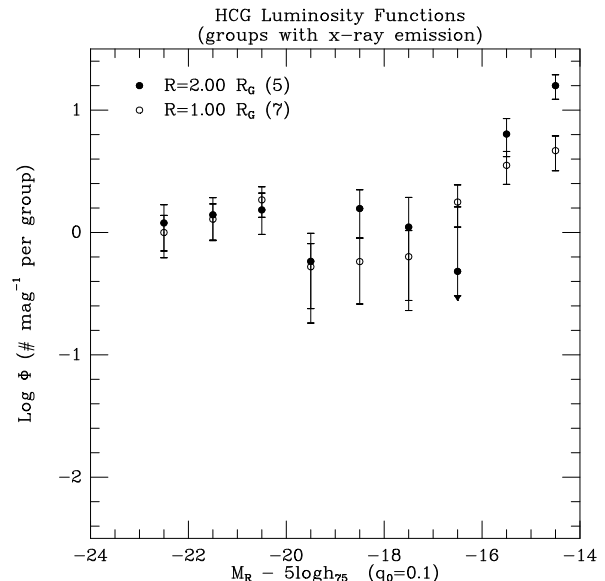


Fig. 12b.— COMPARISON OF LUMINOSITY FUNCTIONS OF X-RAY EMITTING GROUPS WITHIN DIFFERENT RADII. As in the case of groups with dominant ellipticals, there is a significant dwarf population further out from the giant members.

number of groups is shown in parentheses.

Column 2 lists giants per group based on cataloged group members.

Column 3 lists dwarf galaxies per group based on estimated galaxy counts in the magnitude range $-18.0 < M_R - 5 \log h_{75} < -14.0$.

Column 4 lists dwarfs per giant member.

Column 5 shows the result of a generalized χ^2 test which is used to compare the faint end luminosity functions of two subsets.

P_χ evaluates the probability of two data sets being drawn from the same parent population. The calculated values for P_χ indicate that the following subsets are significantly different at the 2σ level: groups with and without tidal dwarfs, groups with dominant ellipticals and with dominant spirals, groups with and without diffuse x-rays, and groups with number of giant members above and below

the median. The difference due to number of giant members is likely related to other properties: the groups with more than 4 giants tend to have dominant ellipticals or diffuse x-rays. If groups with x-ray emission are not included, then the faint end luminosity functions of groups with low and with high M/L measurements are also statistically different. In fact, for groups without diffuse x-rays and with high M/L, a dwarf galaxy population is not detected.

Finally, we want to compare to other luminosity functions. Because of different normalizations, comparing faint end slopes is not necessarily meaningful; we prefer to examine quantities such as dwarf galaxies per group or dwarfs per giant galaxy. There are also problems which arise when comparing luminosity functions with data taken in different filters and at different limiting magnitudes. In some sense, B and R filters select objects with different stellar populations at each magnitude and at the faintest magnitudes, objects detected in one band might not be detected in another. One can assume a universal color in order to compare luminosity functions in different bands, but galaxy colors such as $B - R$ can vary by more than a magnitude depending on morphological type (Fukugita et al. 1995). Because we use a statistical method for counting galaxies, we do not identify individual galaxy members and it becomes impractical to compare our luminosity function in R to a luminosity function produced with B -band data. The other major difficulty is handling different completeness limits. For example, many field luminosity functions are produced from surveys which cover a large area of the sky but are not faint enough to probe the regime of dwarf galaxies. One option is to extrapolate the Schechter function

fit but if there is an upturn at fainter magnitudes that is not being seen, then the reported faint end slope does not represent the dwarf galaxy population we wish to compare. Another option is to perform a comparison based only on galaxy counts within the “brighter” completeness limit. In this case, we may not be including a significant part of the dwarf galaxy population and so a term like “dwarfs per giant” seems inappropriate.

Considering these limitations, we examine various luminosity functions as candidates for comparison. We find no suitable field luminosity functions: the luminosity functions of the Stromlo-APM Redshift Survey (Lovday et al. 1992), the CfA Redshift Survey (Marzke et al. 1994), and the Durham/UKST Galaxy Redshift Survey (Ratcliffe et al. 1998) are based on blue or Zwicky magnitudes and although the luminosity function for the Las Campanas Redshift Survey (Lin et al. 1996) is presented in Gunn- r , the Schechter function fit extends only to $M = -17.5 + 5 \log h$. We would also like to compare to the previous compact group luminosity function of Zepf et al. (1997) but it uses B -band magnitudes and perhaps more importantly, they recalculate group radii so that our respective samples cover very different areas with respect to the giant member galaxies. It is easier to find candidates for comparison among the many cluster luminosity functions. Secker et al. (1997) present a luminosity function in R for the core of the Coma Cluster which extends well beyond the completeness limit needed for a suitable comparison to our luminosity function of compact group galaxies. Based on the luminosity function shown in Figure 9 of the Secker et al. (1997) paper, we calculate a dwarf to giant galaxy ratio $\sim 4.2 \pm 0.5$ for Coma. This value is more than double the

number of dwarfs per giant in the “typical” compact group but it is comparable to the dwarfs per giant in compact groups with diffuse x-ray emission. We further note that the general shape of the Coma luminosity function (Secker et al. 1997, Trentham 1998, Jorgensen & Hill 1997) is similar to that of HCG galaxies. There is a slight dip at intermediate luminosities and then a sharp upturn creating a faint end with a steep slope. Such behavior is also seen in the rich cluster Abell 665 (Wilson et al. 1997).

5. Summary & Discussion

Summarizing, we find that

- Dwarf galaxies are detected in Hickson compact groups using a statistical method for background subtraction. The resultant luminosity function compiled from all groups is not described by a single Schechter function. When we fit the distribution with a composite of two Schechter functions (for bright and faint galaxies), we find that the faint end slope is $\alpha = -1.17$, down to a limiting magnitude of $M_R = -14.0 + \log h_{75}$.
- The general shape of the luminosity function exhibits a dip at $M_R = -17.5 + \log h_{75}$ and $\alpha = -0.52$ for the Schechter function characterizing the bright galaxy population. The decreasing number of galaxies per magnitude with decreasing luminosity suggests a “deficit” of intermediate luminosity galaxies in comparison to most field luminosity functions ($\alpha \sim 1.0$).
- Dwarf galaxies presently observed in tidal debris (tidal dwarf candidates) make

a small contribution to the total luminosity function of all groups, but groups with tidal dwarfs have a significantly larger dwarf population than those without tidal dwarfs.

- Groups with first-ranked E/S0 galaxies have an excess faint galaxy population over those with first-ranked spirals.
- Groups with diffuse x-ray emission have a large dwarf population extending to two group radii. Of the 14 groups with dominant E/S0 galaxies, five of them also have detected x-ray halos.
- The dwarf-to-giant ratio in compact groups with x-ray halos is comparable to that of the cores of rich clusters.

To understand these results, we hypothesize the following (realizing that these are not unique interpretations of the data):

1) *X-ray halos are an indication of previous or current giant galaxy interactions.*

A hot intra-group medium is characterized by extended, diffuse x-ray emission rather than discrete sources which are associated with individual galaxies. Both Ebeling et al. (1994) and Pildis et al. (1995) detected extended x-ray emission in HCGs and discovered a relationship between x-ray emission and the morphological type of the dominant galaxy, i.e., an x-ray group usually has a first-ranked E or S0 galaxy. They also reported an anti-correlation between the spiral fraction of the group and the presence of an x-ray halo. A more complete survey of HCGs by Ponman et al. (1996) finds x-ray emission in some spiral-rich groups as well. Recall that five of the seven x-ray groups in our sample have first-ranked E/S0 galaxies and a low spiral fraction ($< 50\%$) and the other two are spiral-

rich and currently interacting as evidenced by tidal tails. If one assumes that elliptical and lenticular galaxies are merger remnants, then this naturally suggests a connection between interactions/mergers and x-ray halos. During the merger process, gas and stars from the outer spiral disks are being tidally stripped. Supernovae from tidally-triggered star formation and shock-heating in tidal tails may be responsible for heating the gas to x-ray temperatures. Models of merging galaxies (Mihos et al. 1998) indicate that low-mass or extended galaxy halos allow tidal debris to be expelled to large distances.

2) *Many dwarf galaxies form in tidal debris during interactions.*

There is observational and theoretical evidence to support the idea of dwarf galaxy formation in the tidal debris of giant galaxy interactions (cf §1). In a previous paper (Hunsberger et al. 1996), we compiled a list of tidal dwarf candidates for our sample of HCGs using FOCAS detections coincident with tidal features. We identified 47 possible tidal dwarfs in seven of the groups. These tidal dwarfs are responsible for the excess of faint galaxies in Figure 11b, but the real question is what is the ultimate fate of these objects? Elmegreen et al. (1993) predict that if the perturbing galaxy has a greater mass, the tidal dwarfs will be ejected into the group at large or become satellites of the new galaxy instead of falling back into the merger remnant. Therefore, we expect a large fraction of these systems to survive.

Next, consider the similarity of the luminosity functions of groups with tidal dwarfs and groups with diffuse x-ray emission. Neither luminosity function exhibits the deficit of intermediate luminosity galaxies, and both have significant dwarf galaxy populations. If x-ray

halos are a sign of recent interaction and if tidal dwarfs are expelled from giants and can survive for as long as the cooling timescale of the gas then tidal dwarfs provide a reasonable explanation for the abundant dwarf population observed in x-ray groups.

3) *The size and distribution of dark matter halos profoundly affects the evolution of groups of galaxies, especially the dwarf population.*

If individual galaxies have massive halos then mergers occur quite quickly because of dynamical friction (Barnes 1985). If the galaxies have low-mass halos then they present smaller cross-sections for interaction so that the merger rate within the group is slower. In general, as the mass fraction of a common group halo increases, the merger rate decreases (Bode et al. 1993). The mass distribution of a group halo changes as the group evolves. As mergers occur in the central region, the galaxies' orbital energy is transferred to the halo causing it to become less centrally concentrated. Is the dark matter in compact groups in individual galaxy halos or a common group halo? The high spatial density of galaxies in compact groups makes it unlikely that a member can retain an extended halo. The M/L measurements for each HCG listed in Table 2 are based on velocity dispersions of a few giant galaxy members in each group which introduces considerable inaccuracy. Such estimates are meaningful only within the group radius and high M/L values can mistakenly be inferred from large velocity differences of galaxies viewed in projection. Furthermore, it is quite possible that compact groups are not virialized systems. Although the reported mass-to-light ratios may be unreliable, we proceed with a hypothetical discussion. If a group has a low

M/L , i.e., below the median, then galaxies have low-mass halos and either a) there is a low-mass group halo or b) the common halo is more massive but extended and not centrally concentrated. In this situation, giant galaxy interactions can produce tidal tails (Mihos et al. 1998) and tidal debris (and tidal dwarfs) can be ejected into an intra-group medium. In the case of b), the expelled gas should trace the gravitational potential which is now shallow but more extended and be detectable as a diffuse x-ray halo. When a group has a high M/L it means that a) the galaxies have massive halos, b) there is a massive, extended group halo, or c) the common halo is less massive but has a strong central concentration. For a) or c), the massive halo(s) prevent formation of tidal tails during an interaction (Mihos et al. 1998). So as dwarfs are either cannibalized by massive galaxy halos or destroyed during a merger of giant members, there is no way to replenish the population.

4) *There exists some mechanism which preferentially eliminates intermediate luminosity galaxies.*

First we examine what is known about compact group formation. Previous studies hint at a connection between compact groups and loose groups. Despite the original isolation criterion for HCG selection, Ramella et al. (1994) report that 29 of 38 HCGs are embedded in rich, looser systems. N-body simulations (Diaferio et al. 1994) suggest that compact configurations resembling HCGs are continually forming during the collapse of rich loose groups. Furthermore, a plot of group magnitude vs. group diameter (Sulentic & Rabaça 1994) for both loose groups from the CfA survey (Geller & Huchra 1983) and HCGs shows a very smooth transition in parameter space from one sample to the other.

If a compact group evolves from a looser system, then its initial population should be similar to giant field galaxies and their companions.

Statistical analyses of the distribution of satellites around giant galaxies (Lorrimer et al. 1994, Loveday 1997) indicate that faint companions are more strongly clustered about the primary galaxy than their brighter counterparts. It is not clear whether a variation of clustering strength or of galaxy counts is responsible for the lack of intermediate luminosity objects in the luminosity function of compact group galaxies, but in either case, “dynamical friction” offers a plausible explanation.

In the field and loose groups, giant galaxies have companions orbiting within large dark matter halos. Dynamical friction provides a means to decrease the orbital angular momentum of satellites and the timescale for energy loss is inversely proportional to satellite mass. Because the orbits of more massive companions decay more rapidly, they merge sooner with the primary galaxy. If luminosity is proportional to mass, then such a scenario is consistent with fewer bright companions than faint companions, especially near a giant. Recall, however, that the dip in the luminosity function is less severe for groups with tidal dwarfs and essentially disappears for groups with x-ray halos. (As an aside here, we note that 18% of the groups in our total sample are groups with diffuse x-rays while 36% of the Ribeiro et al. (1994) sample are x-ray groups. This may explain why the trough is not a strong feature in their luminosity function.) Is it possible that tidal dwarfs replenish the population of intermediate luminosity galaxies ($-19 < M_R < -17$) and/or that formation of an x-ray halo in-

hibits cannibalism? The tidal dwarf formation models of Barnes & Hernquist (1992) and Elmegreen et al. (1993) predict masses in the range 10^7 to $10^9 M_\odot$. For $M/L = 1$, this corresponds to $-18.2 \leq M_R \leq -13.2$ which agrees with the magnitude range of tidal dwarf candidates in our sample (see Fig. 10a). The tidal dwarf galaxies cataloged by Duc & Mirabel (1998) exhibit a magnitude range of $-18.8 \leq M_B \leq -12.1$ with a median value of $M_B = -14.2$ implying that most tidal dwarfs are low luminosity objects although a few could be considered intermediate luminosity galaxies. Now assume that diffuse x-rays trace a common dark matter halo which is less concentrated than individual galaxy halos (as discussed previously). Because the dynamical friction timescale is inversely proportional to medium density, the loss of orbital energy proceeds more slowly. Once a significant group potential forms, merging times increase as well as the expected lifetimes of dwarf members.

5) *Groups with first-ranked E/S0 galaxies are more evolved than other compact groups, i.e., they have undergone previous mergers.*

In groups with a first-ranked E/S0 galaxy, there is a substantial population of dwarf galaxies which extends out to two group radii (Figure 12b). A possible explanation is that the dwarfs exist “at large” in the group and an example of such a free-floating dwarf population is reported in the Virgo cluster (Ferguson 1992). A merger scenario can explain how the dwarf population gets redistributed and enhanced. Assume that a dominant-spiral compact group is evolving into a dominant-E/S0 group. Initially dwarfs are bound to individual galaxies and their distribution traces the giant galaxy halos. As two giant members merge, some of the dwarf companions

are destroyed, but more importantly the dark matter is restructured. It becomes less centrally concentrated and more extended, either creating a common group halo or making the existing one more massive. If tidal tails form during the interaction and if they are sites of dwarf galaxy formation (tidal dwarfs), then there is a mechanism by which the dwarf population can be replenished and enhanced. The conditions which allow tidally stripped gas to form a hot (x-ray emitting) intra-group medium may also distribute tidal dwarfs throughout the group. When such a merger is complete, the distribution of both the hot x-ray gas and the dwarf population will trace the extended group halo. This scenario is consistent with results from a survey of twelve poor groups, including three HCGs, conducted by Zabludoff & Mulchaey (Zabludoff & Mulchaey 1997, Mulchaey & Zabludoff 1997). They discovered that nine x-ray detected groups had 20 – 50 dwarf members ($-16 < M_B - 5 \log h < -14$) and established that groups with a central elliptical have an x-ray halo extending $100 - 300 h^{-1} \text{kpc}$. They concluded that the longevity of the dwarf members is increased because of the distribution of dark matter in an extended common halo.

Finally, combining these hypotheses, we speculate that the evolution of a typical HCG may proceed as follows: The group forms because dynamical friction of massive dark halos around field galaxies brings them together. These newly formed HCGs contain dwarf companions to the giant galaxies, but these are gradually cannibalized as interactions occur. Eventually a major merger occurs and this has several consequences: the formation of a giant E/S0 galaxy, the production of an x-ray halo, and the formation

of tidal dwarfs. The ongoing interactions strip gas, dark matter, and dwarf companions from the giants and spread them into a common group halo. This redistribution extends the lifetime of the dwarf population (and the group as a whole) and creates an environment more conducive to the tidal dwarf replenishment process.

We would like to thank M. Bershady, C. Churchill, R. Ciardullo, J. Feldmeier, J. Hibbard, and P. Hickson for their helpful comments. SDH and JCC acknowledge financial support from NSF grant AST-9529242. DZ acknowledges financial support from an NSF grant (AST-9619576), a NASA LTSA grant (NAG-5-3501), the David and Lucile Packard Foundation, and the Alfred P. Sloan Foundation.

REFERENCES

- Barnes, J. 1985, MNRAS, 215, 517
- Barnes, J. E. & Hernquist, L. 1992, Nature, 360, 715
- Bode, P. W., Cohn, H. N., & Lugger, P. M. 1993, ApJ, 416, 17
- Diaferio, A., Geller, M. J., & Ramella, M. 1994, AJ, 107, 868
- Duc, P.-A. & Mirabel, I. F. 1994, A&A, 289,83
- Duc, P.-A. & Mirabel, I. F. 1998, to be published in Proceedings of IAU Symposium 186
- Ebeling, H., Voges, W., & Boehringer, H. 1994, ApJ, 436, 44
- Elmegreen, B. G., Kaufman, M., & Thomasson, M. 1993, ApJ, 412, 90
- Ferguson, H. C. 1992, MNRAS, 255, 389
- Ferguson, H. C. & Sandage, A. 1991, AJ, 101, 765
- Fukugita, M., Shimasaku, K., & Ichikawa, T. 1995, PASP, 107, 945
- Geller, M. J. & Huchra, J. P. 1983 ApJS, 52, 89
- Heiligman, G. M. & Turner, E. L. 1980 ApJ 236, 745
- Hernquist, L., Katz, N. S., & Weinberg, D. H. 1995, ApJ, 442, 57
- Hickson, P. 1982, ApJ, 255, 382
- Hickson, P., Kindl, E., & Auman, J. R. 1989, ApJS, 70, 687
- Hickson, P., Mendes de Oliveira, C., Huchra, J. P., & Palumbo, G. G. 1992, ApJ, 399, 353
- Hunsberger, S. D., Charlton, J. C., & Zaritsky, D. 1996, ApJ, 462, 50
- Jarvis, J. F. & Tyson, J. A. 1981, AJ, 86, 476
- Jorgensen, I. & Hill, G. J. 1997, BAAS, 29, 5, 105.07
- Landolt, A. U. 1992, AJ, 104, 340
- Lin, H., Kirshner, R. P., Shectman, S. A., Landy, S. D., Oemler, A., Tucker, D. L., & Schechter, P. L. 1996, ApJ, 464, 60
- Lorrimer, S. J., Frenk, C. S., Smith, R. M., White, S. D. M., & Zaritsky, D. 1994 MNRAS 269, 696
- Loveday, J. 1997 ApJ, 489, 29

- Loveday, J., Peterson, B. A., Efstathiou, G., & Maddox, S. J. 1992, *ApJ*, 390, 338
- Mamon, G. A. 1990, in *Paired and Interacting Galaxies*, ed. J. W. Sulentic, W. C. Keel, & C. M. Telesco (Washington: NASA), 619
- Marzke, R. O., Huchra, J. P., & Geller, M. J. 1994, *ApJ*, 428, 43
- Mendes de Oliveira, C. & Hickson, P. 1991, *ApJ*, 380, 30
- Mendes de Oliveira, C. & Hickson, P. 1994, *ApJ*, 427, 684
- Mihos, C., Dubinski, J., & Hernquist, L. 1998, *ApJ*, 494, 183
- Mirabel, I. F., Dottori, H., & Lutz, D. 1992, *A&A*, 256, L19
- Mirabel, I. F., Lutz, D., & Maza, J. 1991, *A&A*, 243, 367
- Mulchaey, J. S. & Zabludoff, A. I. 1997, *ApJ*, in press
- Pildis, R. A., Bregman, J. N., & Evrard, A. E. 1995, *ApJ*, 443, 514
- Ponman, T. J., Bourner, P. D. J., Ebeling, H., & Bohringer, H. 1996, *MNRAS*, 283, 690
- Ramella, M., Diaferio, A., Geller, M. J., & Huchra, J. P. 1994, *AJ*, 107, 1623
- Ratcliffe, A., Shanks, T., Parker, Q. A., & Fong, R. 1998, *MNRAS*, 293, 197
- Ribeiro, A. L. B., de Carvalho, R. R., & Zepf, S. E. 1994, *MNRAS*, 267, L13
- Schechter, P. 1976, *ApJ*, 203, 297
- Secker, J., Harris, W. E., & Plummer, J. D. 1997, *PASP*, 109, 1377
- Sulentic, J. W. & Rabaça, C. R. 1994, *ApJ*, 429, 531
- Trentham, N. 1998, *MNRAS*, 293, 71
- Tyson, J. A. 1988, *AJ*, 96, 1
- Wilson, G., Smail, I., Ellis, R. S., & Couch, W. J. 1997, *MNRAS*, 284, 915
- Zabludoff, A. I. & Mulchaey, J. S. 1997, *ApJ*, in press
- Zepf, S. E., de Carvalho, R. R., & Ribeiro, A. L. 1997, *ApJL*, 488, 11
- Zwicky, F. 1956, *Ergebnisse der Exakten Naturwissenschaften*, 29, 344

TABLE 1
COMPLETENESS LIMITS

HCG	z	R	M_R
001	0.0339	21.50	-14.19
003	0.0255	21.10	-13.97
004	0.0280	21.00	-14.27
005	0.0410	21.50	-14.61
006	0.0379	20.70	-15.24
007	0.0141	21.70	-12.07
012	0.0485	20.80	-15.68
013	0.0411	21.50	-14.62
014	0.0183	21.20	-13.14
016	0.0132	21.20	-12.42
020	0.0484	21.60	-14.88
024	0.0305	21.30	-14.16
025	0.0212	21.70	-12.96
026	0.0316	21.30	-14.24
028	0.0380	21.50	-14.44
030	0.0154	21.60	-12.36
031	0.0137	21.50	-12.21
032	0.0408	21.20	-14.90
033	0.0260	21.10	-14.01
034	0.0307	21.40	-14.07
037	0.0223	21.60	-13.17
038	0.0292	20.60	-14.76
040	0.0223	21.30	-13.47
043	0.0330	21.40	-14.23
046	0.0270	21.10	-14.09
047	0.0317	20.50	-15.04
049	0.0332	21.30	-14.35
051	0.0258	21.70	-13.39
052	0.0430	20.50	-15.72
056	0.0270	21.30	-13.89
089	0.0297	21.00	-14.40
092	0.0215	20.90	-13.79
094	0.0417	21.40	-14.75
095	0.0396	20.80	-15.24
096	0.0292	21.60	-13.76
097	0.0218	20.80	-13.92
098	0.0266	21.00	-14.16
099	0.0290	21.20	-14.15
100	0.0178	21.60	-12.68

TABLE 2
 PROPERTIES OF OBSERVED COMPACT GROUPS

HCG #	N	First Ranked	Spiral Frac	M/L h^{-1}	Vel Disp (km/s)	Median Sep (h^{-1} kpc)
001*	4	S	1/4	15	85	49.0
003	3	S	2/3	363	251	77.0
004	3	S	1/3	229	339	57.0
005	3	S	1/3	20	148	25.7
006	4	S0	2/4	60	251	25.1
007	4	S	4/4	14	89	45.6
012†	5	S0	2/5	74	240	58.9
013	5	S	1/5	39	182	46.8
014	3	S	2/3	27	331	26.9
016*†	4	S	2/4	22	123	44.6
020	5	S0	0/5	78	275	31.4
024	5	S0	2/5	40	200	29.5
025	4	S	2/4	9	62	47.9
026*	7	S	1/7	71	200	31.6
028	3	S	1/3	7	85	21.9
030	4	S	3/4	11	72	51.3
031*	3	S	2/3	1	66	8.1
032	4	E	1/4	41	209	61.7
033†	4	E	1/4	46	155	24.5
034	4	E	2/4	100	316	15.5
037†	5	E	2/5	123	398	28.8
038*	3	S	2/3	—	13	58.9
040	5	E	3/5	15	148	15.1
043	5	S	4/5	155	224	58.9
046	4	E	1/5	479	324	39.8
047	4	S	3/4	1	43	36.3
049	4	S	2/4	—	34	12.3
051†	5	E	2/5	72	240	58.9
052	3	S	3/3	110	182	87.1
056	5	S	2/5	26	170	21.4
089	4	S	4/4	7	55	58.9
092*†	4	S	4/4	44	389	28.2
094	7	E	1/7	159	479	57.5

TABLE 2—*Continued*

HCG #	N	First Ranked	Spiral Frac	M/L h^{-1}	Vel Disp (km/s)	Median Sep (h^{-1} kpc)
095	4	E	3/4	50	309	30.2
096*	4	S	2/4	15	132	30.2
097†	5	E	2/5	348	372	63.1
098	3	S	1/3	23	120	27.5
099	5	S	2/5	50	263	42.7
100	3	S	3/3	32	89	38.0

* indicates a group containing tidal dwarf candidates (Hunsberger et al. 1996)

† indicates a group with diffuse x-ray emission (Ponman et al. 1996)

TABLE 3
COMPACT GROUP POPULATIONS

Subset Description	Giants per Group	Dwarfs* per Group	Dwarfs per Giant	P_x^\dagger
all groups [‡]				
$R = 1.00R_G$ (39)	4.2	5.7 ± 0.8	1.4 ± 0.2	
$R = 1.25R_G$ (39)	4.2	6.5 ± 1.0	1.5 ± 0.2	
$R = 1.50R_G$ (39)	4.2	7.2 ± 1.1	1.7 ± 0.3	
$R = 1.75R_G$ (37)	4.2	7.2 ± 1.4	1.7 ± 0.3	
$R = 2.00R_G$ (34)	4.1	5.4 ± 1.5	1.3 ± 0.4	
R=25kpc (39)	4.2	1.1 ± 0.3	0.3 ± 0.1	
R=50kpc (39)	4.2	3.4 ± 0.7	0.8 ± 0.2	
R=75kpc (38)	4.2	5.9 ± 1.0	1.4 ± 0.2	
R=100kpc (35)	4.3	5.4 ± 1.4	1.3 ± 0.3	
R=125kpc (32)	4.3	6.7 ± 1.9	1.6 ± 0.4	
R=150kpc (27)	4.2	-1.6 ± 2.9	-0.4 ± 0.7	
with tidal dwarfs [‡] (7)	4.1	11.4 ± 2.3	2.8 ± 0.6	0.013
without tidal dwarfs (32)	4.2	6.2 ± 1.3	1.5 ± 0.3	
with 1st-ranked E/S0 (14)	4.7	11.5 ± 2.4	2.4 ± 0.5	0.012
with 1st-ranked S (25)	3.9	3.7 ± 1.3	0.9 ± 0.3	
with x-ray emission (7)	4.6	15.0 ± 2.8	3.3 ± 0.6	< 0.001
without x-ray emission (32)	4.1	3.4 ± 1.2	0.8 ± 0.3	
$M/L < 50h^{**}$ (21)	3.9	5.7 ± 1.3	1.5 ± 0.3	0.535
$M/L \geq 50h$ (16)	4.6	7.1 ± 2.3	1.5 ± 0.5	
velocity dispersion < 200km/s ^{**} (20)	3.8	5.4 ± 1.4	1.4 ± 0.4	0.744
velocity dispersion > 200km/s (19)	4.5	6.7 ± 1.9	1.5 ± 0.4	
spiral fraction < 50% (19)	4.6	7.7 ± 2.1	1.7 ± 0.5	0.729
spiral fraction \geq 50% (20)	3.8	5.2 ± 1.4	1.4 ± 0.4	

TABLE 3—*Continued*

Subset Description	Giants per Group	Dwarfs* per Group	Dwarfs per Giant	P_χ^\dagger
median separation $< 39h^{-1}\text{kpc}^{**}$ (20)	4.1	5.4 ± 1.3	1.3 ± 0.3	0.355
median separation $> 39h^{-1}\text{kpc}$ (19)	4.3	6.5 ± 1.9	1.5 ± 0.4	
# giant members ≤ 4 (26)	3.6	3.5 ± 1.3	1.0 ± 0.4	0.004
# giant members > 4 (13 ^{††})	5.3	10.8 ± 2.1	2.0 ± 0.4	
groups without x-ray emission				
$M/L < 50h$ (18)	3.9	5.1 ± 1.4	1.3 ± 0.4	0.028
$M/L \geq 50h$ (12)	4.5	-3.9 ± 2.7	-0.9 ± 0.6	

* Dwarf galaxy counts include objects in the luminosity range $-18.0 < M_R < -14.0$ within $R = 1.50R_G$ unless otherwise stated.

† Calculated values are based on a comparison of faint end data points of the appropriate luminosity functions. A value of P_χ approaching zero implies the two data sets are from different populations.

‡ Tidal dwarf candidates are included only in these subsets.

** This is the median value of the Hickson catalog.

†† We note that 8 of the 13 groups have dominant E/S0 galaxies and/or x-ray halos.